International Journal of Nanomedicine

Dovepress

open access to scientific and medical research

Open Access Full Text Article

ORIGINAL RESEARCH

Combination of PEI-$Mn_{0.5}Zn_{0.5}Fe_2O_4$ nanoparticles and pHsp 70-*HSV-TK*/GCV with magnet-induced heating for treatment of hepatoma

This article was published in the following Dove Press journal:
International Journal of Nanomedicine
18 November 2015
Number of times this article has been viewed

Qiusha Tang[1]
Mudan Lu[2]
Daozhen Chen[2]
Peidang Liu[1]

[1]School of Medicine, Southeast University, Nanjing, [2]Genetic Laboratory, Wuxi Hospital for Maternal and Child Health Care, the Affiliated Hospital of Nanjing Medical University, Wuxi, People's Republic of China

Background: To explore a new combination of thermal treatment and gene therapy for hepatoma, a heat-inducible herpes simplex virus *thymidine kinase*/ganciclovir (*HSV-TK*/GCV) gene therapy system was developed in which thermal energy generated by $Mn_{0.5}Zn_{0.5}Fe_2O_4$ nanoparticles (MZF-NPs) under an alternating magnetic field was used to activate gene expression.

Methods: First, a recombinant eukaryotic plasmid, pHsp 70-*HSV-TK*, was constructed as a target gene for therapy. This recombinant plasmid was used to transfect SMMC-7721 hepatoma cells and the gene expression was evaluated. Magnet-induced heating was then applied to cells to assess the antihepatoma effects of the polyethylenimine (PEI)-MZF-NPs/pHsp 70-*HSV-TK*/GCV complex, in vitro and in vivo.

Results: The results showed that cells were successfully transfected with pHsp 70-*HSV-TK* and that expression levels of *HSV-TK* remained stable. Both in vitro and in vivo results indicated that the combination of gene therapy and heat treatment resulted in better therapeutic effects than heating-alone group. The rates of apoptosis and necrosis in the combined treatment group were 49.0% and 7.21%, respectively. The rate of inhibition of cell proliferation in the combined treatment group was significantly higher (87.5%) than that in the heating-alone group (65.8%; $P<0.01$). The tumor volume and mass inhibition rates of the combined treatment group were 91.3% and 87.91%, respectively, and were significantly higher than the corresponding rates of the heating-alone group (70.41% and 57.14%; $P<0.01$). The expression levels of Stat3 and Bcl-xL messenger RNA and p-Stat3 and Bcl-xL protein in the combined treatment group were significantly lower than those in the other groups ($P<0.01$). The expression levels of Bax messenger RNA and protein in the recombinant plasmid group were significantly higher than those in the other groups ($P<0.01$).

Conclusion: It can therefore be concluded that the combined application of heat treatment and gene therapy has a synergistic and complementary effect and that PEI-MZF-NPs can simultaneously act both as a nonviral gene vector and a magnet-induced source of heat, thereby representing a viable approach for the treatment of cancer.

Keywords: $Mn_{0.5}Zn_{0.5}Fe_2O_4$ nanoparticles, heat-inducible gene expression, hyperthermia, gene therapy, *HSV-TK*/GCV, SMMC-7721 hepatoma cells

Correspondence: Qiusha Tang
School of Medicine, Southeast University, Dingjiaqiao Road 87, Nanjing 210009, Jiangsu Province, People's Republic of China
Tel +86 25 8327 2373
Fax +86 25 8327 2541
Email panyixi-tqs@163.com

Introduction

The recent development of plasmid technology has partially addressed the concern of the safety of gene therapy, in addition to resolving the technical issue of the efficiency of transfection of exogenous genes.[1] Many highly effective cloning vectors have been established for the transfection of various mammalian cell lines deemed appropriate for clinical gene transfection research. Controlling the expression of a target gene

in vivo has been demonstrated to be a critical factor for the success of gene therapy.[2–4] In current methods of gene therapy, uncontrollable gene expression occurs when target genes are automatically activated by a viral promoter or the vector itself. This overexpression or inappropriate expression can distort the outcome of gene therapy. Moreover, it may cause fatal results, as in the case of insulin gene therapy for diabetes and other gene therapies employing cytokines, such as tumor necrosis factor alpha and interleukin-12.[5–7] These issues raise the question of how to effectively control the expression of exogenous genes in vivo, at a level that mimics their natural temporal and spatial expression. Such questions must be answered prior to embarking upon a clinical trial for a particular gene therapy. Among various inducible gene expression methods, those that rely upon external physical factors are more favorable, because target gene expression occurs according to a specified time and spatial order. It has been reported that both γ radiation and the Egr-1 promoter can induce target gene expression.[8–10] However, due to bodily injury caused by ionizing radiation, radiation therapy has limited clinical application.

Hyperthermia is a highly recommended, noninvasive, and nontoxic therapy method.[11] The application of heat induces a specific promoter, which in turn induces specific target gene expression in a designated tissue.[12] Many hyperthermic methods have been used to induce gene expression to date. For example, Huang et al[12] demonstrated that in cultured cells, the expression of a heterologous gene with a heat shock protein 70 (Hsp 70) promoter could be elevated to 500- to 1,000-fold greater than background expression by use of a hot water bath (39°C–43°C). However, this method cannot be easily applied to gene therapy in vivo, due to the challenge of heating specific areas within the human body to the desired temperatures.

In 1997, German scholars Jordan et al[13] used nanotechnology combined with magnetic induction thermotherapy (magnetic fluid hyperthermia [MFH]) to effectively treat a tumor, thus providing a novel application for MFH. Not only do tumor cells absorb nanomagnetic materials at a high rate (8- to 400-fold greater than normal cells), but they also distribute these materials evenly into descendent cells. Tumor cells containing nanomagnetic particles are easily killed by MFH,[14,15] which is also known as intracellular thermotherapy. This method is target-oriented, that is, increased temperatures occur only in tumor tissues with magnetic particles, and does not affect normal tissues not containing magnetic particles.

Along with the development of nanotechnology, studies on nanomagnetic particles as gene transfer carriers have been performed.[16–18] In previous research,[19,20] we developed a novel heat-inducible gene expression system in which thermal energy generated by Mn–Zn ferrite magnetic nanoparticles (MZF-NPs) under an alternating magnetic field was used to activate gene expression. There were four main advantages to this system: 1) utilization of the relatively low Curie point of MZF-NPs to control the in vivo hyperthermia temperature and therefore achieving safe and effective heat-inducible transgene expression;[21,22] 2) use of the promoter of HSPs that are conserved among species from bacteria to humans. It has been shown that promoters of some HSPs can activate gene expression by several 1,000-fold in response to moderate hyperthermia;[23] 3) in addition to the simplicity of preparation of magnetic nanocarriers, there is no associated cellular toxicity, and surface modification confers on them very high biocompatibility;[24] 4) gene carriers can physically aggregate rapidly at the target site and with the help of mechanical external forces, carrier concentration is significantly increased, thus removing the main barriers to low gene expression efficiency (slow aggregation of the carrier at the target site and insufficient carrier concentration carrier at the target site[25]). In conclusion, it is possible to control target gene expression profile via use of the combination of the Hsp 70 promoter and heating.

Based on preliminary findings from our previous study[20] attempts were made to develop a heat-inducible herpes simplex virus thymidine kinase/ganciclovir (*HSV-TK*/GCV) gene therapy system in which thermal energy generated by MZF-NPs under an alternating magnetic field was used to activate gene expression. Out of several new methods of gene therapy that have been explored for the treatment of cancer, the *HSV-TK*/GCV system demonstrates the highest efficacy for targeted gene therapy.[26] In this system, thymidine kinase, a suicide gene expressed by *HSV-TK*, converts the nontoxic drug precursor GCV into a toxic drug, which kills tumor cells undergoing rapid growth by penetrating cells and inhibiting DNA synthesis. This system also produces a toxic effect on adjacent, untransfected cancer cells, via the bystander effect. In general, if 10% of target cells are transfected and therefore express the gene of interest, the therapeutic toxic effect will extend to the remainder of the tumor tissue via mechanisms related to gap junctions and apoptosis.[27,28] Because this class of enzymes does not exist in mammals, the precursor drug exhibits very low toxicity or is nontoxic to mammalian cells.

In this study, we first constructed a recombinant eukaryotic plasmid, pHsp 70-*HSV-TK*, as a target gene for therapy. Next, this recombinant plasmid was used to transfect SMMC-7721 hepatoma cells in vitro and in vivo. This system was used to explore a new therapy for hepatoma via a combination of

thermal treatment and gene therapy, using polyethylenimine (PEI)-coated MZF-NPs (PEI-MZF-NPs) as the gene transfection vector and magnet-induced media simultaneously. Here, we provide evidence that this combined therapy offers a new strategy for the treatment of cancer.

Materials and methods

Plasmids and reagents

pHSV-106, which harbors the herpes simplex virus type I thymidine kinase gene (*HSV-TK*), was donated by Professor Lu Daru (Life Sciences Institute of Fudan University, Shanghai, People's Republic of China); pD3SX (11.1 kb), a mammalian expression vector containing the Hsp 70 promoter was obtained from Stressgen Bioreagents Corp. (Victoria, BC, Canada); PEI (average mW 25 kDa, average degree of polymerization 580) and most of the reagents were purchased from Sigma-Aldrich (St Louis, MO, USA); MagnetoFACTOR plates were purchased from Chemicell (Berlin, Germany). Anti-Bax antibody, anti-Bcl-xL antibody, anti-p-Stat3 antibody, and anti-β-actin antibody were purchased from Immuno Way (Newark, DE, USA). Total RNA extraction kit, reverse transcription kit, high-purity gel extraction kit, SYBR® Premix Ex Taq™ polymerase chain reaction (PCR) kit, and DNA marker were obtained from Takara Biotechnology Co. Ltd. (Dalian, Shiga, Japan).

Construction and identification of the eukaryotic expression plasmid pHsp 70-*HSV-TK*

PCR amplification of *HSV-TK* segments

HSV-106 plasmids were used as templates, and *HSV-TK* fragments were amplified by PCR. The restriction enzyme site *Sal*I was introduced into the primers. The primer sequences were as follows: Forward, 5′-GGTCGACCTTGTAGAAG CGCGTATGGC-3′ and Reverse, 5′-CGGTCGACCGGTA TTGTCTCCTTCCGTG-3′.

The *Sal*I restriction enzyme site sequence was GTC GACC and the product length was 1,168 bp.

Construction of recombinant pHsp 70-*HSV-TK* plasmid

The *HSV-TK* fragments were collected, amplified, and subcloned into pD3SX at *Sal*I sites. After transformation, the pHsp 70-*HSV-TK* recombinant plasmid was purified and identified by electrophoresis of the PCR product. PCR primers were:

Forward: 5′-CAGCAGCCTCCGTGGCCTCCAGCAT CCGACAAG-3′ (located at pD3SX);

Reverse: 5′-CGGTCGACCGGTATTGTCTCCTTCC GTG-3′.

Identification of recombinant pHsp 70-*HSV-TK* plasmid by restriction enzyme digestion and DNA sequencing

Recombinant pHsp 70-*HSV-TK* plasmid was restriction digested by the *Sal*I enzyme, and correct insertion was confirmed by agarose gel electrophoresis. Uncut pHsp 70-*HSV-TK* plasmid, uncut pD3SX plasmid, and digested pD3SX plasmid served as controls. A 10 μL sample of purified recombinant pHsp 70-*HSV-TK* plasmid was dispatched to Shanghai Shengong Co. (Shanghai, People's Republic of China) for complete DNA sequencing.

Preparation and characterization of Mn–Zn ferrite nanoparticles and PEI-coated Mn–Zn ferrite nanoparticles

Mn–Zn ferrite nanoparticles and PEI-MZF-NPs were prepared and characterized as described previously.[19,20,24]

Cell lines and establishment of tumors in nude mice

SMMC-7721 cells were provided by the Institute of Biochemistry and Cell Biology, Shanghai Institute of Biological Sciences, Chinese Academy of Sciences, Shanghai, People's Republic of China. All experiments involving use of human cells were performed under the approval of the ethics committee of Southeast University, Nanjing, People's Republic of China. SMMC-7721 cells were cultured in Dulbecco's Modified Eagle's Medium (DMEM, Gibco Life Technologies, New York, NY, USA), supplemented with 10% fetal bovine serum (HyClone, GE Healthcare Life Sciences, Pittsburgh, PA, USA), streptomycin (100 mg/mL), and penicillin (100 U/mL). All cells were incubated at 37°C in a humidified atmosphere of 5% CO_2. Cells were passaged, using trypsin/ethylenediaminetetraacetic acid medium, when almost confluent.

BALB/C nude mice (male, 10 weeks of age) were purchased from the Lakes Animal Experimental Centre of the Institute of Biochemistry and Cell Biology, Shanghai Institute of Biological Sciences, Chinese Academy of Sciences. Animal experiments were approved by the Animal Care Committee of Jiangsu Province and were performed in accordance with the Principles of Laboratory Animal Care formulated by the National Society for Medical Research and the Guide for the Care and Use of Laboratory Animals prepared by the Institute of Laboratory Animal Resources and published by the National Institutes of Health.[29] All mice were maintained

in the Sterile Barrier System of the Medical School, Southeast University, Nanjing, People's Republic of China.

SMMC-7721 cells (1×10^7) were subcutaneously transplanted into the right shoulder blades of nude mice. Tumor-bearing mice were randomized for study when tumors grew to 5mm^3 in size. These mice were housed in a special pathogen-free animal facility. All animal experiments were carried out in compliance with the national laws related to the conduct of animal experimentation.

Antihepatoma effects in vitro

Testing expression of *HSV-TK* by reverse transcription-(RT)-PCR

Before transfection, pHsp 70-*HSV-TK* and PEI-MZF-NPs were diluted separately in serum- and supplement-free medium. Then, 8 μg of pHsp 70-*HSV-TK* per well were mixed with PEI-MZF-NPs (20 mg/mL) to form a complex, at an N/P ratio of 5, in a final volume of 800 μL of serum- and supplement-free medium. The complexes were incubated at room temperature for 30 minutes. SMMC-7721 cells were seeded in 60 mm dishes at an initial density of 6×10^5 cells/well in 5 mL of growth medium. After incubation for 18 hours (to reach 80% confluence at the time of transfection), the medium was replaced with 4.2 mL serum-free medium with 800 μL complexes and incubated for a further 15 minutes on a MagnetoFACTOR plate. The medium was exchanged for fresh medium containing serum prior to incubation.

After incubation for 24 hours, MZF-NPs at 10 g/L final concentration were added, followed by exposure of SMMC-7721/*TK* (thymidine kinase) cells to a high-frequency alternating electromagnetic field (*F*=230 kHz, *I*=28 A), and irradiation for 60 minutes; 72 hours later, total RNA was extracted from SMMC-7721/*TK* cells. As a control, total RNA of the SMMC-7721 parent cells was also extracted. Infected cells that were not exposed to hyperthermia were also used as controls. Each experiment was carried out in triplicate.

Glyceraldehyde 3-phosphate dehydrogenase (*GAPDH*) cDNA was used as an internal reference gene. All reagents and consumables used to extract RNA were ribonuclease (RNase)-free or were soaked in diethylpyrocarbonate-treated water. Primer sequences are listed in Table 1. A two-step RT-PCR method was used to amplify the genes. Gel electrophoresis (2% agarose) was used to identify the correct products.

Table 1 Primer sequences of PCR

Gene	Primer fragment	Length (bp)
HSV-TK	F: 5′-AGCATCCGACAAGAAGCTC-3′ R: 5′-GCTATGCTGGCTGCGATTC-3′	496
Stat3	F: 5′-TGTCTAAAGGTCCCTCATC-3′ R: 5′-CCATAGTGTGCATCATGTC-3′	104
Bcl-xL	F: 5′-CAGGTATGGAAGGGTTTG-3′ R: 5′-TAGGGATGGAAGGAAAGG-3′	233
Bax	F: 5′-CCATCTTTGTGGCGGGAGTG-3′ R: 5′-TTGTGTCCCGAAGGAGGTTTATTAC-3′	222
GAPDH	F: 5′-CACCCACTCCTCCACCTTTG-3′ R: 5′-CCACCACCCTGTTGCTGTAG-3′	110

Abbreviations: *Bax*, bcl-2 associated X protein; *Bcl-xL*, B-cell lymphoma-extra large; bp, base pair; *GAPDH*, glyceraldehyde 3-phosphate dehydrogenase; PCR, polymerase chain reaction; *Stat3*, signal transducer and activator of transcription 3; F, forward; R, reverse.

Testing expression of *HSV-TK* by Western blot

Proteins from the aforementioned groups were extracted in lysis buffer (RIPA; Shengong, Shanghai, People's Republic of China). Proteins were separated by 10% sodium dodecyl sulfate polyacrylamide gel electrophoresis and transferred onto polyvinylidene fluoride membranes. After washing, the membranes were blocked with 5% skimmed milk at room temperature for 1 hour, incubated with anti-TK antibodies (1:200 dilution) or anti-*GAPDH* antibody (1:1,000, final dilution) at 4°C overnight, then incubated with secondary antibody for 1 hour. Bound antibody was detected using enhanced chemiluminescence (Thermo Pierce ECL Western Blotting Substrate; Thermo Scientific, Rockford, IL, USA) and quantified using Image J software (Gel-Pro analyzer 4.0; Media Cybernetics, Inc., Rockville, IL, USA) Gel-pro Analyzer.

Treatment groups

After transfection as described earlier and incubation for 24 hours, SMMC-7721/*TK* cells and SMMC-7721 cells were digested, and then cells were seeded in four culture bottles, grouped as: a) the untransfected SMMC-7721 cells group, which served as a blank control; b) the gene transfection-alone group (without heating); c) the thermotherapy-alone group (without transfection); and d) gene therapy combined with heating therapy group (with transfection and heating).

Twenty-four hours later, GCV at 5 μg/mL final concentration was added to the groups (b) and (d). PEI-MZF-NPs at 10 g/L final concentration were added to the groups (c) and (d). An identical volume of DMEM culture medium was added to the blank control group. The thermal therapy bottles (groups [c] and [d]) were exposed to a high-frequency alternating electromagnetic field (*F*=230 kHz, *I*=28 A), and irradiated for 60 minutes.

MTT assay of cell growth and proliferation

Incubation of all groups was continued for 48 hours, after which 20 μL of MTT(3-(4,5-dimethyl-2-thiazolyl)-2,

5-diphenyl-2-H-tetrazolium bromide) solution (5 g/L in phosphate-buffered saline [PBS]) were added to each well, and the cells were further incubated at 37°C for 4 hours. To each well of the 96-well plate, 150 μL of dimethyl sulfoxide were added to solubilize the formazan crystals, followed by reading of the optical density (OD) at 492 nm using a spectrophotometer (Bio-Tek; BioTek Instruments, Inc., Winooski, VT, USA). Readings of six wells were measured for each group. The following formula was used to calculate the cell growth inhibition rate (IR): IR = (1− the experimental group OD/the negative control group OD) ×100%.

Flow cytometry assay

Cells (2×10^6) were harvested from each group. After washing with PBS, supernatants from each group were removed and cell pellets were resuspended in 100 mL Annexin-V-FLUOS labeling solution containing 2 mL of Annexin-V-FLUOS and 2 mL of propidium iodide (PI). Cells were incubated for 15 minutes without light at 25°C, then analyzed on a flow cytometer (FCM, Vantage SE; Becton, Dickinson and Company, Franklin Lakes, NJ, USA) within 1 hour.

Cell morphology

For electron microscopy, cells (5×10^6) were collected and centrifuged at 2,500× *g* for 10 minutes, fixed in 4% glutaraldehyde at 4°C for 72 hours and washed with PBS. They were then fixed in 1% osmium tetroxide, dehydrated stepwise using acetone after washing with PBS, embedded in EPON 812 (Sigma-Aldrich) after permeation, and converged for 12 hours at 35°C, for 24 hours at 45°C, and for 24 hours at 60°C in turn. Finally, cells were prepared as ultrathin sections (60 nm), stained with uranyl acetate and lead citrate, then viewed using a transmission electron microscope (TEM/model Hitachi 750; Hitachi High Technologies Ltd., Tokyo, Japan).

Animal experiments

Experimental groups and treatment

When tumor diameters reached approximately 0.5 cm, mice were divided into four groups of ten mice each: a) the untransfected SMMC-7721 cells group, which served as a blank control; b) the gene transfection-alone group (without heating); c) the thermotherapy-alone group (without transfection); and d) gene therapy combined with heating therapy group (with transfection and heating).

The method of transfection was as follows: pHsp 70-*HSV-TK* and PEI-MZF-NPs were diluted separately in saline solution. Before transfection, 20 μg of pHsp 70-*HSV-TK* per nude mouse were mixed with PEI-MZF-NPs magnetic fluid (20 mg/mL) to form a complex, at an N/P ratio of 5, in a final volume of 200 μL of saline. Then, complexes were incubated at room temperature for 30 minutes. Following a multipoint injection strategy, moving clockwise at the 3, 6, 9, and 12 o'clock positions, 200 μL of complexes were injected into the tumors.

The method of hyperthermia treatment was as follows: 0.046 mL of MZF-NPs MF (net magnetite weight: 4.6 mg) was multipointed infiltrative injected into the tumors, which were then subjected to hyperthermia treatment for 60 minutes. The tumor temperature was measured at multiple points using an infrared thermometer (UMI, FISO Technologies Inc., Saint–Foy, QC, Canada).

For groups (b) and (d), gene transfection was performed once per week, while 100 mg GCV/kg intraperitoneal injections were performed every day. For groups (c) and (d), hyperthermia treatment was performed once every 3 days. For group (a), 200 μL of sterile normal saline were injected intraperitoneally every day.

Mice were sacrificed after 6 weeks, and the mass and volume of each tumor were measured. Tumor growth inhibition was evaluated by measuring mass and volume inhibition proportions. Mass inhibition was calculated as (1− relative tumor mass) ×100%, where relative tumor mass was the mean tumor mass of the experimental group divided by the mean tumor mass of the blank control group. Similarly, volume inhibition was calculated as (1− relative tumor volume) ×100%, where relative tumor volume was the mean tumor volume of the experimental group divided by the mean tumor volume of the blank control group.

Expression of *HSV-TK* in vivo

Total RNA was extracted from the aforementioned groups, both for evaluation of the expression of *HSV-TK* as described in "Testing expression of *HSV-TK* by reverse transcription (RT)-PCR" section". PCR products were separated on 2% agarose gel by electrophoresis and visualized by ethidium bromide staining.

Real-time PCR assay

To quantify the *Stat3*, *Bcl-xl*, and *Bax* messenger RNA (mRNA) expression, quantitative PCR was performed. Real-time PCR was performed using the SYBR® Premix Ex Taq™ PCR kit (Takara Biotechnology Co. Ltd.) on the Applied Biosystems 7300 Real-Time PCR System (Foster, CA, USA). The 20 μL reaction of the SYBR Green assay contained 10 μL of 2× SYBR Premix Ex Taq, 0.4 μL PCR forward primers and 0.4 μL reverse primers, 0.4 μL ROX

reference dye (50×), 2 μL cDNA, and 6.8 μL double-distilled H_2O. PCR was carried out as follows: one cycle of 95°C for 10 minutes, and 40 cycles of three steps (95°C for 5 seconds, 60°C for 45 seconds, and 72°C for 30 seconds). Data were normalized to *GAPDH* and calculated using the ΔΔCt method.[30] Primer sequences are listed in Table 1.

Western blot immunoassay

The *p-Stat3*, *Bcl-xL*, and *Bax* proteins levels were determined by a protein imprinting method (Western blot). Proteins from the aforementioned groups were extracted in lysis buffer (RIPA, shenggong, shanghai People's Republic of China). Proteins were separated by 10% sodium dodecyl sulfate polyacrylamide gel electrophoresis and transferred onto polyvinylidene fluoride membranes. After washing, the membranes were blocked with 5% skimmed milk at room temperature for 1 hour, incubated with anti-*p-Stat3*, anti-*Bax*, or anti-*Bcl-xL* antibodies (1:1,000 dilution) or anti-*β-actin* antibody (1:1,000, final dilution) at 4°C overnight, then incubated with secondary antibody for 1 hour. Bound antibody was detected using enhanced chemiluminescence (Thermo Pierce ECL Western Blotting Substrate; Thermo Scientific) and quantified using ImageJ software (Gel-Pro analyzer 4.0; Media Cybernetics, Inc.; Rockville; USA). Data were normalized to loading control and expressed as relative *p-Stat3*, *Bcl-xL*, and *Bax* proteins levels compared to corresponding control.

Immunohistochemistry analysis in vivo

To further examine the heating effects on the tumor, an immunohistochemical analysis of tumors was performed. The tumor sections were first probed with a polyclonal rabbit anti-mouse apoptosis regulator Bax (Bcl-2-associated X protein) antibody (1:400) at 4°C overnight, followed by incubation with biotinylated polyclonal goat anti-rat antibody (1:200), in a humidified chamber for 1 hour, and were then immersed in 0.3% H_2O_2 in absolute methanol for 15 minutes to block endogenous peroxidase. In succession, the sections were counterstained with hematoxylin and mounted with glass coverslips, and were visualized in an optical microscope.

Statistical analysis

All values are expressed as mean ± standard deviation. Student's *t*-test was used to identify significant differences between groups. Values of $P<0.05$ were considered statistically significant. All tests were performed using SPSS software (version 13.0; SPSS Inc., Chicago, IL, USA).

Results and discussion

Identification of the pHsp 70-*HSV-TK* plasmid

Identification of pHsp 70-*HSV-TK* by PCR

PCR amplification of the *HSV-TK* gene segment was carried out using pHSV-106 plasmid as a template. The PCR product was electrophoresed on a 10 g/L agarose gel, which resulted in a gene segment of 1,168 bp (Figure 1).

Identification of pHsp 70-*HSV-TK* by restriction enzyme digestion

It was expected that digestion of the constructed pHsp 70-*HSV-TK* gene with *Sal*I would generate a *HSV-TK* fragment of 1,168 bp. As shown in Figure 2, agarose gel electrophoresis of pHsp 70-*HSV-TK* digested with *Sal*I clearly showed a band of ~1,168 bp in lane 2, which corresponded to the recombinant plasmid pHsp 70-*HSV-TK*.

Identification of pHsp 70-*HSV-TK* by DNA sequencing

According to the *HSV-TK* sequence data from DNASTAR and GenBank, the PD3sx-98 was the correct clone, the

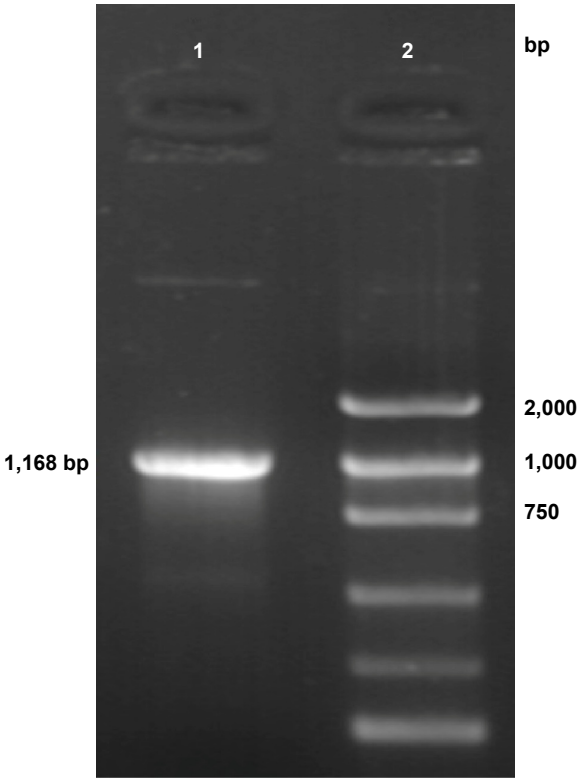

Figure 1 PCR amplification of *HSV-TK* gene from the pHSV-106 plasmid.
Notes: Lane 1, *HSV-TK* gene PCR amplification products; lane 2, marker (each band in turn from bottom to top is 100, 300, 500, 750, 1,000, and 2,000 bp).
Abbreviations: bp, base pair; *HSV-TK*, herpes simplex virus thymidine kinase; PCR, polymerase chain reaction.

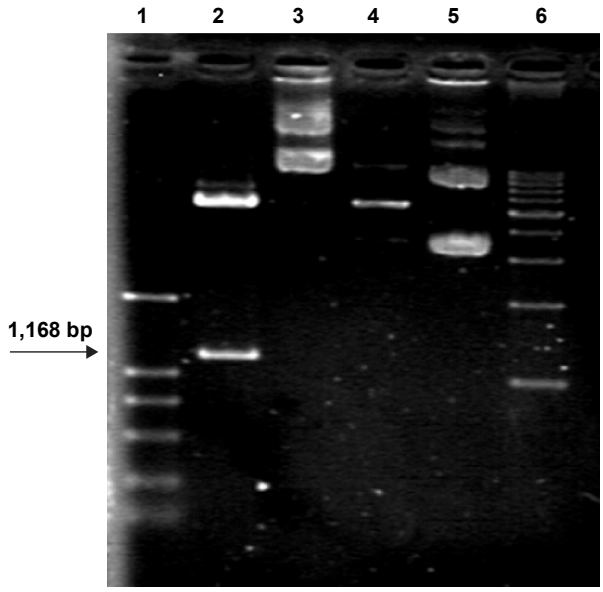

Figure 2 pHsp 70-*HSV-TK* was identified by restriction enzyme digestion.
Notes: Lane 1, marker (each band in turn from bottom to top is 100, 300, 500, 750, 1,000, and 2,000 bp); lane 2, pHsp 70-*HSV-TK* was cut by *SalI*; lane 3, pHsp 70-*HSV-TK* was not cut by any restriction endonucleases; lane 4, pD3SX was cut by *SalI*; lane 5, pD3SX was not cut by any restriction endonucleases; lane 6, marker (each band in turn from bottom to top is 1,000, 2,000, 3,000, 4,000, 5,000, 6,000, 7,000, and 8,000 bp).
Abbreviations: bp, base pair; *HSV-TK*, herpes simplex virus thymidine kinase.

HSV-TK gene segment was successfully inserted into pD3SX, and the inserted DNA sequence was 100% accurate.

Gene integration of *HSV-TK* in SMMZ-7721 cells mediated by PEI-MZF-NPs

Expression of *HSV-TK* mRNA in SMMC-7721 cells transfected with PEI-MZF-NPs was evaluated by RT-PCR. The *GAPDH* gene was used as an internal control to rule out any operational error in the PCR process and to determine the quality of *HSV-TK* cDNA. As shown in Figure 3, RT-PCR using mRNA from SMMC-7721 cells transfected and heated display two distinct genetic fragments of 496 bp and 110 kb, which corresponded to the lengths of *HSV-TK* and *GAPDH*, respectively. Only a band at 110 kb (corresponding to *GAPDH*) was detected in the SMMC-7721 cells without transfection. Furthermore, there is also only a band at 110 kb (corresponding to *GAPDH*) in the transfected SMMC-7721cells that did not receive heating. These results suggested that SMMC-7721 cells were successfully transfected with pHsp 70-*HSV-TK* mediated by PEI-MZF-NPs, and that the gene expression was activated by MFH.

Expression of TK proteins in SMMC-7721 cells transfected with PEI-MZF-NPs was evaluated by Western blot. The *GAPDH* gene was used as an internal control. As shown in Figure 4, proteins from SMMC-7721 cells

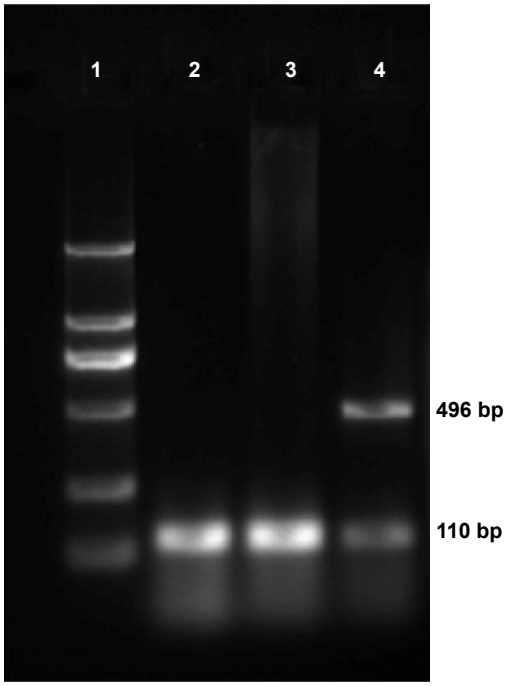

Figure 3 Gel electrophoresis of HSV-*TK* amplified by RT-PCR after pHsp 70-*HSV-TK* transfected into SMMC-7721 cells.
Notes: Lane 1, marker (each band in turn from bottom to top is 100, 300, 500, 750, 1,000, and 2,000 bp); lane 2, infected cells that did not receive hyperthermia with only one strip, 110 bp of *GAPDH*; lane 3, untransfected SMMC-7721 cells with only one strip, 110 bp of *GAPDH*; lane 4, infected cells that receive hyperthermia with two clear strips, 496 bp of HSV-*TK* and 110 bp of *GAPDH* used as reference gene.
Abbreviations: bp, base pair; *GAPDH*, glyceraldehyde 3-phosphate dehydrogenase; *HSV-TK*, herpes simplex virus thymidine kinase; RT-PCR, reverse transcription-polymerase chain reaction.

transfected and heated display two distinct band of 26 and 36 kDa, which corresponded to the protein expression of *HSV-TK* and *GAPDH*, respectively. Only a band at 36 kDa (corresponding to *GAPDH*) was detected in the SMMC-7721 cells without transfection. Furthermore, there is also only a band at 36 kDa (corresponding to *GAPDH*) in the transfected SMMC-7721cells that did not receive heating. These results suggested that SMMC-7721 cells were successfully transfected with pHsp 70-*HSV-TK* mediated by PEI-MZF-NPs, and that the gene expression was activated by MFH.

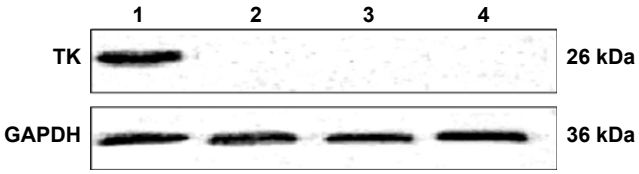

Figure 4 Western blot analysis of thymidine kinase (TK) protein expression. TK =26 kDa; GAPDH =36 kDa.
Notes: Lane 1, blank control; lane 2, gene transfection-alone group; lane 3, the thermotherapy-alone group; lane 4, the combined therapy group.
Abbreviation: GAPDH, glyceraldehyde 3-phosphate dehydrogenase.

In vitro therapeutic effects on SMMC-7721 cells

Inhibition of SMMC-7721 cell proliferation was assessed by MTT

The effect of *HSV-TK*/GCV gene therapy combined with hyperthermia on the proliferation of SMMC-7721 cells for 48 hours was determined by MTT assay. As shown in Table 2, cytotoxic effects were increased in the group treated with combined *HSV-TK*/GCV gene therapy and hyperthermia compared with the other groups, with an IR of 87.5%. By contrast, the IR value for the thermotherapy-alone group was 65.8%. The difference in cytotoxic effect between the *HSV-TK*/GCV gene therapy combined with hyperthermia group compared with the other groups was statistically significant ($P<0.01$). These data suggested that the combination of *HSV-TK*/GCV gene therapy with hyperthermia was more effective in inhibiting cell proliferation than hyperthermia alone.

As far as the gene therapy-alone group is concerned, the IR value was 1.97%. The difference in cytotoxic effect between the gene therapy-alone group compared with the control group was not statistically significant ($P>0.05$). These data suggested that the gene therapy-alone group has no cytotoxic effect because the gene expression was not activated by MFH.

Flow cytometric analysis of apoptosis

SMMC-7721 cells were stained with Annexin-V and PI and analyzed by flow cytometry to determine whether growth inhibition induced by various treatments was caused by apoptosis or necrosis. Generally speaking, in the early stages of apoptosis, changes occur only at the cell surface. One such alteration is the translocation of phosphatidylserine (PS) from the inner part of the plasma membrane to the outer layer, exposing PS at the cell's external surface, which can be detected by Annexin-V staining. Since PS is also exposed in necrotic cells according to the loss of membrane integrity, apoptotic cells must be differentiated from necrotic cells. The simultaneous application of a DNA stain, PI, which is used for dye exclusion tests, stains only necrotic cells, thus allowing discrimination between these two cell types.

As shown in Table 3 and Figure 5, both apoptotic and necrotic cells were present in all treatment groups, with apoptotic cells being the major constituent. The group in which gene therapy and thermal treatment were combined exhibited the highest efficacy; the rates of apoptosis and necrosis in this group were 49.0% and 7.21%, respectively. By contrast, the rates were 14.49% and 9.62% in the thermotherapy-alone group, 1.53% and 0.11% in the gene therapy-alone group, and 1.04% and 0.07% in the blank control group.

Cell ultrastructural examination

SEM examination revealed that the cells of control group and gene transfection-alone group have rather regular shape with intact nuclei, fine chromatin, and a large, clear nucleolus; and the characteristic features of normal cell surface such as numerous microvilli and lamellipodia extensions are shown in Figure 6A and B. By contrast, in the pHsp 70-*HSV-TK* gene combined heat treatment group and thermotherapy-alone group, the cell membrane and organelles disintegrated into pieces. SMMC-7721 cells were observed to exhibit morphological features typical of apoptotic cells, such as chromatin condensation and chromatin margination or cleavage, and apoptotic body formation (Figure 6C and D). Scattered or flake-gathered high electron density materials are visible in the combined treatment group cells (Figure 6E).

In vivo therapeutic effects on SMMC-7721 cells

Gene integration of *HSV-TK* mediated by PEI-MZF-NPs

Tumors from all treatment groups were excised 24 hours after hyperthermia treatment, and total RNA was extracted and subjected to RT-PCR. As shown in Figure 7, two distinct genetic fragments of 496 bp and 110 kb, corresponding to the lengths of *HSV-TK* and *GAPDH*, were observed in the gene

Table 2 SMMC-7721 cell proliferation inhibition rates of different treatments

Groups	OD (mean ± SD, n=6)	Proliferation inhibition (%)
Blank control group	1.52±0.03	NA
Gene transfection-alone group	1.49±0.05[d]	1.97
Thermotherapy-alone group	0.52±0.03[a–c]	65.8
Gene therapy combined with heating therapy group	0.19±0.02[a,b]	87.5

Notes: [a]$P<0.001$ versus the blank control group. [b]$P<0.001$ versus the gene transfection-alone group. [c]$P<0.001$ versus the gene therapy combined with heating therapy group. [d]$P>0.05$ versus the blank control group.
Abbreviations: NA, not applicable; OD, optical density; SD, standard deviation.

Table 3 The apoptotic and necrotic rate (%) of different therapy groups detected by flow cytometric analysis

Groups	AR	NR	Total of apoptosis and necrosis rate
Blank control group	1.04	0.07	1.11
Gene transfection-alone group	1.53	0.11	1.64
Thermotherapy-alone group	14.49	9.62	24.11
Gene therapy combined with heating therapy group	49.00	7.21	56.21

Abbreviations: AR, apoptotic rate; NR, necrotic rate.

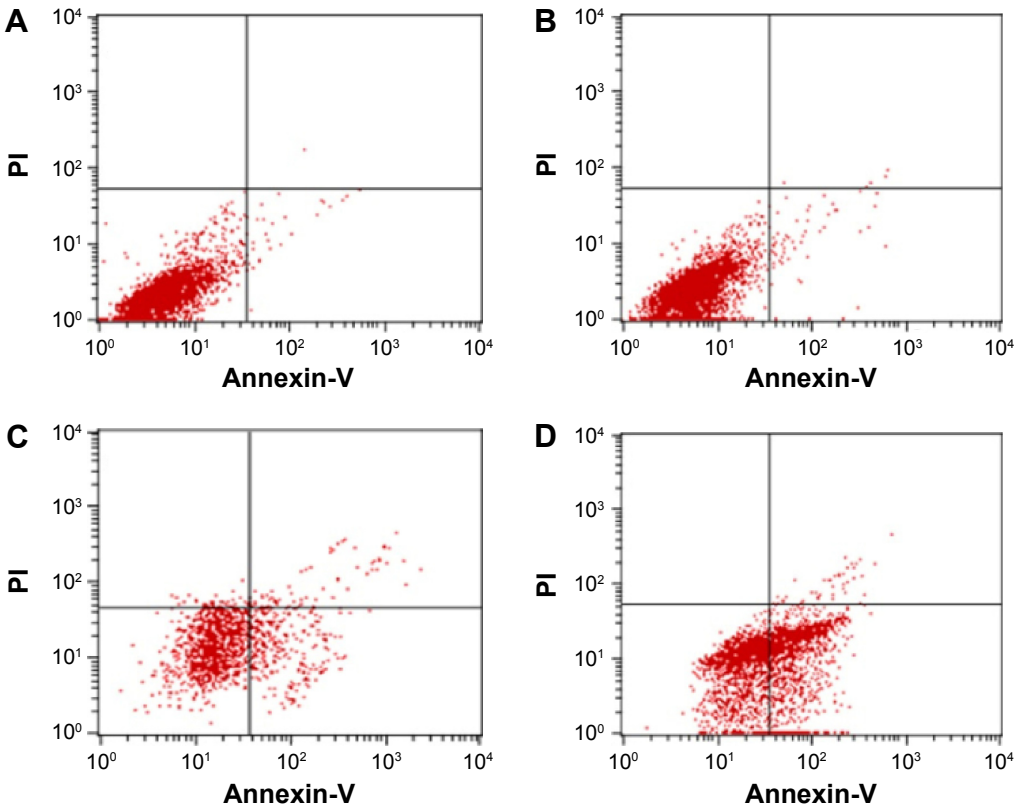

Figure 5 Apoptosis and necrosis of SMMC-7721 cells analyzed by flow cytometry after different treatments.
Notes: (**A**) The blank control group. The AR and NR was, respectively, 1.04% and 0.07%. (**B**) The gene transfection-alone group. The AR and NR was, respectively, 1.53% and 0.11%. (**C**) The thermotherapy-alone group. The AR and NR was, respectively, 14.49% and 9.62%. (**D**) Gene therapy combined with heating therapy group. The AR and NR was, respectively, 49.00% and 7.21%.
Abbreviations: AR, apoptotic rate; NR, necrotic rate; PI, propidium iodide.

transfection combined with hyperthermia treatment group, whereas only a band at 110 kb (*GAPDH*) was observed in the gene transfection-alone group and blank control group. These results suggested that SMMC-7721 cells were successfully transfected with pHsp 70-*HSV-TK*, mediated by PEI-MZF-NPs, and that gene expression was activated by MFH.

In vivo antihepatoma effect

To avoid liquid overflow, to ensure fluid dispersion in tumor tissues, and to transfect the maximum possible number of tumor cells, a multipoint injection strategy was applied, in which MZF-NPs or the PEI-MZF-NPs/pHsp 70-*HSV-TK* complex were injected into each tumor at the 3, 6, 9, and 12 o'clock positions.

As shown in Table 4, tumor growth in nude mice exposed to the combination of gene therapy with heat treatment was inhibited to a greater degree than in those treated with MZF magnetic induction heating treatment alone. The tumor volume and mass IR of group (d) were 91.30% and 87.91%, respectively, significantly higher than the 70.41% and 57.14% of group (c). As far as the gene therapy-alone group is concerned, the tumor volume and mass IR were 0.79% and 1.64%, respectively. The difference between the gene therapy-alone groups compared with the control groups was not statistically significant ($P>0.05$). These data suggested that the gene therapy-alone group has no cytotoxic effect because the gene expression was not activated by MFH.

Histological examination revealed that, in both the pHsp 70-*HSV-TK* gene combined heat treatment group and thermotherapy-alone group, many black nanoparticles accumulated in the stroma of the tumors, with widespread tumor necrosis surrounding the nanoparticles. The necrotic areas of the groups (c) and (d) were larger than those of the control group and gene therapy-alone group (Figure 8).

Bax staining assay was performed here to determine the apoptosis of the cells in the tumor after four different treatments (Figure 9). It indicated that the tumors treated with pHsp 70-*HSV-TK* gene combined heat treatment group and thermotherapy-alone group have the extensive regions of apoptotic cells (Figure 9A and B), and the number of apoptotic cells was significantly more than those of the control group and gene therapy-alone group (Figure 9C and D).

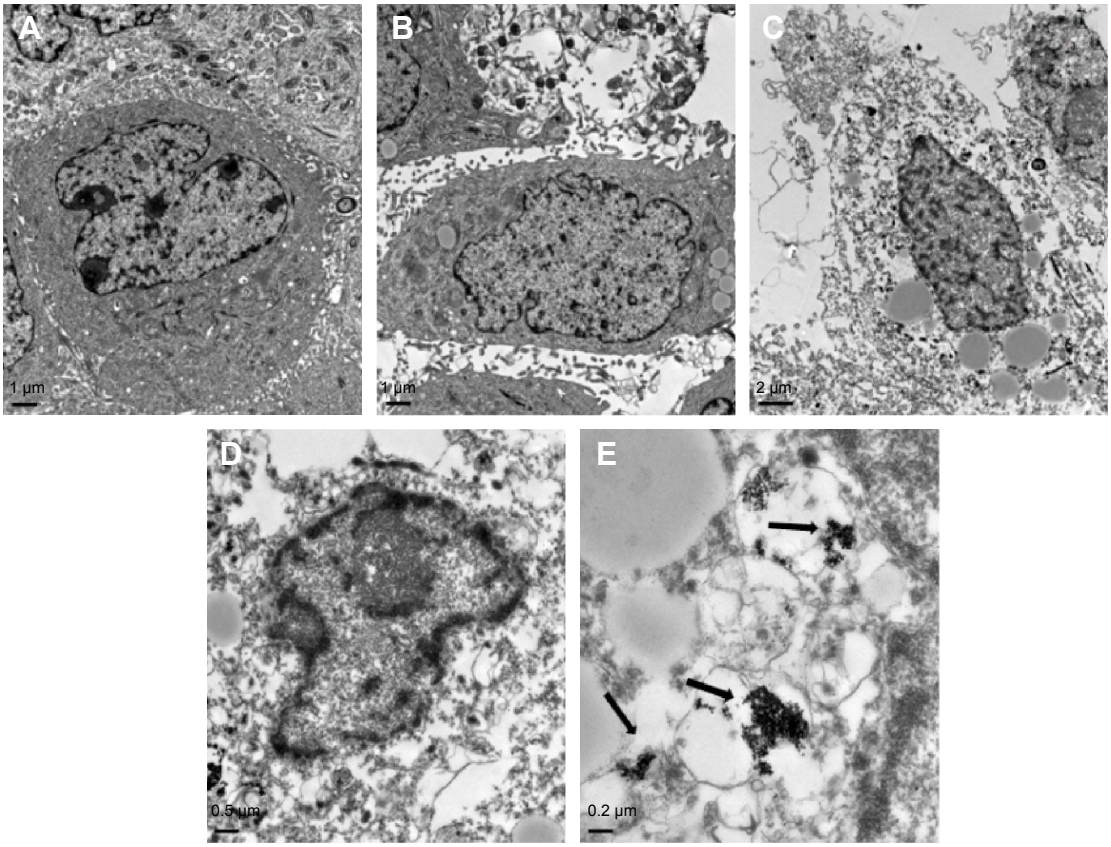

Figure 6 Ultrastructure of SMMC-7721 cells (observed by TEM).
Notes: Sections from the blank control group (**A**); gene transfection-alone group (**B**); thermotherapy-alone group (**C**); and combined therapy group (**D** and **E**) are shown. TEM examination revealed that the necrotic areas in **C** and **D** were much larger than the intrinsic necrosis of the tumor shown in **A** and **B**. The black arrows indicate the magnetic nanoparticles. Magnification: **A**–**C** ×6,000; **D** ×12,000; **E** ×30,000.
Abbreviation: TEM, transmission electron microscopy.

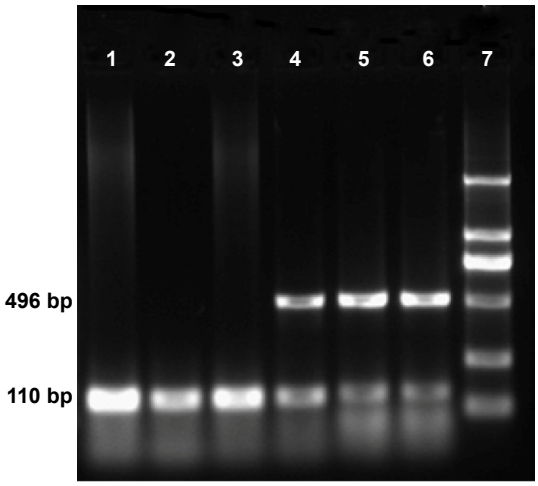

Figure 7 Gel electrophoresis of HSV-*TK* amplified by RT-PCR after pHsp 70-*HSV-TK* transfected into SMMC-7721 cells.
Notes: Lane 1, the thermotherapy-alone group with only one strip, 110 bp of *GAPDH*; lane 2, the gene transfection-alone group with only one strip, 110 bp of *GAPDH*; lane 3, the blank control group with only one strip, 110 bp of *GAPDH*; lanes 4–6, gene therapy combined with heating therapy group with two clear strips, 496 bp of *HSV-TK* and 110 bp of *GAPDH* used as reference gene; lane 7, marker (each band in turn from bottom to top is 100, 300, 500, 750, 1,000, and 2,000 bp).
Abbreviations: bp, base pair; *GAPDH*, glyceraldehyde 3-phosphate dehydrogenase; *HSV-TK*, herpes simplex virus thymidine kinase; RT-PCR, reverse transcription-polymerase chain reaction.

The previous data indicate that the combination of gene therapy and magnetic induction heating on this type of cancer, using MZF magnetic nanoparticles as the link, can achieve a synergistic effect; that is, 1+1>2. Combined therapy is not simply a combination of thermotherapy and *HSV-TK*/GCV suicide gene therapy, but requires their synergism and complementarities.

Over the past few years, hyperthermia has a wide-ranging application in the treatment or adjuvant treatment of malignant tumor, but the ability to kill the tumor cells is limited, hence the application of hyperthermia gradually faded away in recent years. However, with the combination of hyperthermia and gene therapy, not only can target gene play a better therapeutic role, but also it is a good method to reduce the side effects caused by the gene therapy. Therefore this combination therapy method will provide a new way for therapy for cancer or other disease.

Heating can induce gene expression: on the one hand, heat-induced gene expression can increase the lethality of hyperthermia; on the other hand, it can decrease the expression of target gene. Hyperthermia can also enhance the effect of

Table 4 Volume and mass inhibition rates of SMMC-7721 cell in nude mice after different treatments

Groups	Tumor volume (mm^3) (mean ± SD, n=10)	Tumor mass (g) (mean ± SD, n=10)	IR of volume (%)	IR of mass (%)
Blank control group	1,094.99±142.33	0.91±0.12	NA	NA
Gene transfection-alone group	1,103.68±161.46[d]	0.925±0.12[d]	0.79	1.64
Thermotherapy-alone group	323.98±52.09[a–c]	0.39±0.05[a–c]	70.41	57.14
Gene therapy combined with heating therapy group	95.17±23.11[a,b]	0.11±0.01[a,b]	91.30	87.91

Notes: [a]$P<0.001$ versus the blank control group. [b]$P<0.001$ versus the gene transfection-alone group. [c]$P<0.001$ versus the gene therapy combined with heating therapy group. [d]$P>0.05$ versus the blank control group.
Abbreviations: IR, inhibition rate; NA, not applicable; SD, standard deviation.

gene therapy and play a synergistic antitumor effect; the mechanism may be as follows: 1) High temperature may increase the perfusion of capillary, then the distribution of the drug is changed with local drug concentration increasing. 2) High temperature damages the stability of tumor cells, and increases the permeability of the cell membrane, which make it easy for drug entering the cell, raising the intracellular concentration of the drug. 3) High temperature changes the cytotoxicity of the drug. At 37°C, the drug has no cytotoxicity, but at 40°C it shows significant toxicity. 4) Under effective temperature, the synthesis of HSP that induces drug tolerance is decreased, thereby preventing the occurrence of heat tolerance; this situation has been confirmed in the drugs tolerance experiments such as mitomycin, bleomycin, cisplatin, and so on.[31,32] 5) Hyperthermia inhibits DNA damage response mediated by DNA polymerase, which inhibits the repairmen of tumor cells with sublethal damage and potentially lethal damage after injury caused by the chemotherapy drugs.[33] It can also significantly increase the oxygen content of the tumor, and enhance the treatment sensitivity.[34] 6) With the combination of hyperthermia and chemotherapy, apoptosis may occur in more tumor cells.[35] Demonstrated that under the same time and concentration, hyperthermia combinations with paclitaxel was used to treat liver cancer, thermochemotherapy shows

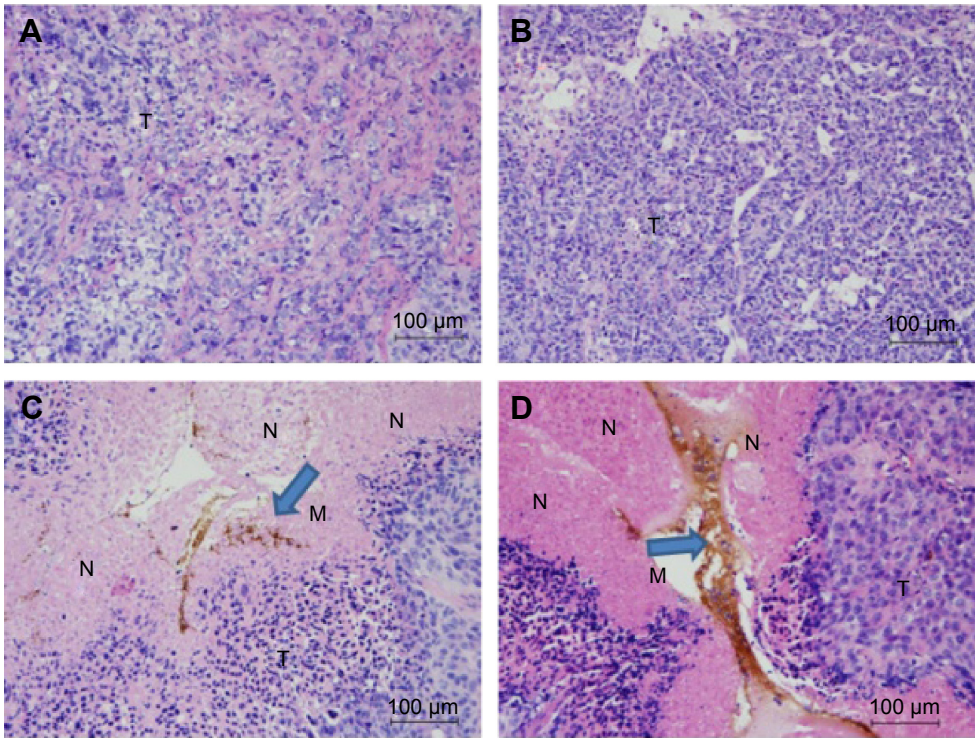

Figure 8 Histological changes in xenograft tumors (H & E).
Notes: Sections from the blank control (**A**); gene transfection-alone group (**B**); thermotherapy-alone group (**C**); and combined therapy group (**D**) are shown. Histological examination revealed that the necrotic areas in **C** and **D** were much larger than the intrinsic necrosis of the tumor shown in **A** and **B**. The blue arrows indicate the magnetic nanoparticles. Magnification ×200.
Abbreviations: H & E, hematoxylin and eosin; M, materials of $Mn_{0.5}Zn_{0.5}Fe_2O_4$ nanoparticles; N, necrosis; T, tumor tissue.

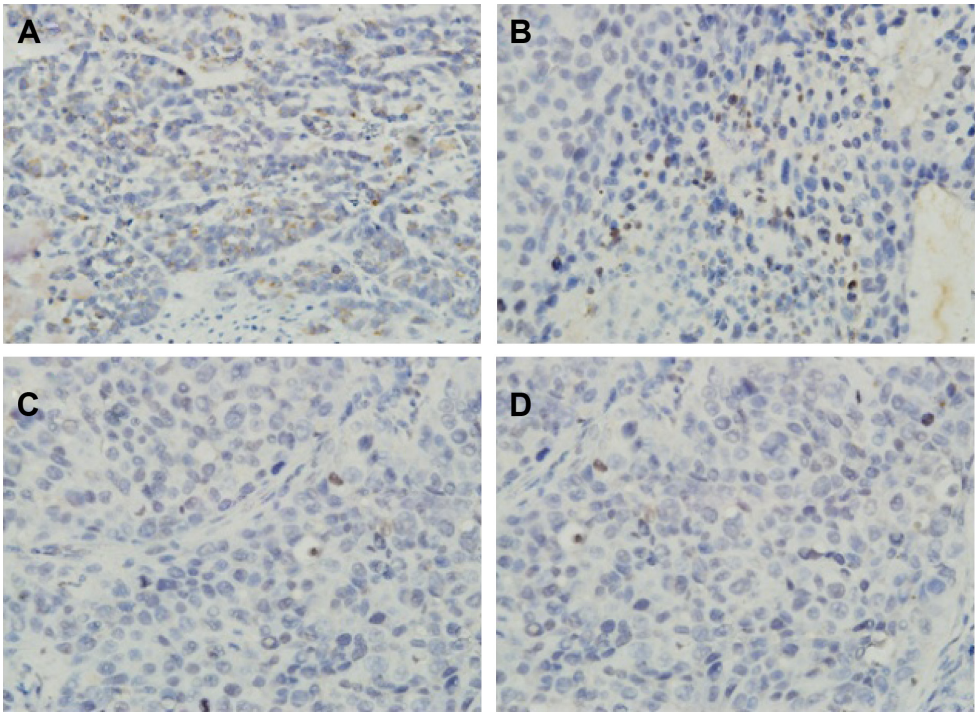

Figure 9 Immunohistochemical staining for Bax.
Notes: Representative immunohistochemical staining with Bax polyclonal antibodies in each group. Apoptosis cells are identified by dark brown (original magnification, ×400). It is evident that the abundance of apoptosis tumor cells is higher in the combined therapy group (**A**) and the thermotherapy-alone group (**B**) than in the gene transfection-alone group (**C**) or blank control (**D**).
Abbreviation: Bax, Bcl-2 associated X protein.

a higher apoptosis rate than the sum of hyperthermia and chemotherapy, the mechanism may be related to the inhibition of the expression of bcl-2 and promoting apoptosis. 7) Hyperthermia can reduce vascular endothelial growth factor synthesized and secreted by tumor, which may lead to the destruction and reduction of tumor angiogenesis.[36] Vascular endothelial cells, unlike tumor cells, are not easy to mutate. Vascular endothelial cells rarely establish resistance, and inhibiting tumor angiogenesis to prevent tumor growth also has a magnifying effect.[37] 8) Blood supply is sufficient in the peripheral portion of the tumor, where the drug is easy to reach, so pharmacologic therapy has advantages on the treatment of peripheral portion. Combining with hyperthermia, the therapeutic effect can cover all tumors.

In summary, in this experiment, we placed promoter Hsp 70 in the upstream of the *TK* gene, and constructed a eukaryotic expression vector pHsp 70-*HSV-TK* induced by heat that can be used to gene therapy and increase the expression of *HSV-TK* gene, thereby the efficiency of killing hepatoma cells are improved. The therapeutic effect of liver cancer is induced by heat and gene therapy, which provide a basis for hyperthermia and gene therapy of liver cancer. This new method of combining gene therapy and hyperthermia is known as gene–hyperthermia therapy, and this method deals with the problems in the practice of hyperthermia or gene therapy alone, which provide a new framework for the treatment of cancer.

Determination of *Stat3*, *Bcl-xL*, and *Bax* expression levels by real-time fluorescent quantitative PCR (real-time PCR) and Western blot immunoassay

Signal transducer and activator of transcription 3 (*Stat3*) is one of the most important members of the signal transducer and activator of transcriptional family (which includes *Stat1–4, Stat5a* and *Stat5b,* and *Stat6*). Constitutive activation of phosphorylated *Stat3* induces the expression of the antiapoptotic genes *Bcl-2, Bcl-xL, survivin, Mcl-1,* and *XIAP*, the cell cycle regulation genes *cyclin D1* and *c-myc* and the angiogenesis-related gene vascular endothelial growth factor. This leads to abnormal cell proliferation, malignant transformation, enhanced tumor resistance to apoptosis, promotion of tumor invasion, metastasis, angiogenesis, and enhanced tumor multidrug resistance by downregulation of the expression of antiapoptotic genes such as *Bax, Bak*, and *Bid*.[38,39] Studies have suggested that the persistent activation of Stat3 plays a key role in resistance to apoptosis of signal transduction pathways in hepatocellular carcinoma.[40,41]

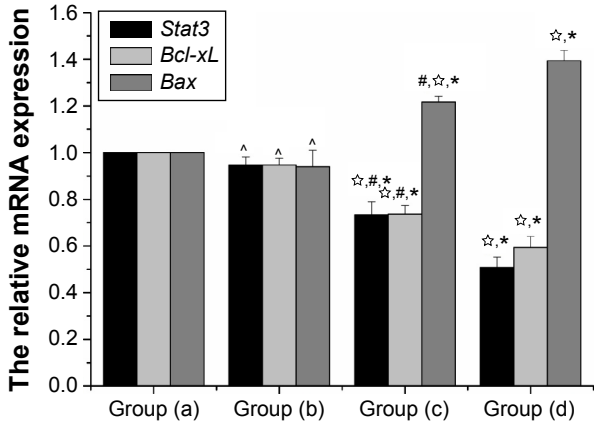

Figure 10 The relative mRNA expression of *Stat3, Bax, Bcl-xL* mRNA was isolated and subjected to quantitative PCR analysis.

Notes: Data were normalized to *GAPDH* levels, data are reported as mean ± standard deviation (N=10), data represent the mean of ten independent experiments each performed in technical triplicate. Group (a), blank control; group (b), gene transfection-alone group; group (c), the thermotherapy-alone group; group (d), the combined therapy group. *$P<0.05$, compared with blank control; ☆compared with gene transfection-alone group; #$P<0.05$, compared with the combined therapy group; ^$P>0.05$, compared with the blank control group.

Abbreviations: *Bax*, bcl-2 associated X protein; *Bcl-xL*, B-cell lymphoma-extra large; *GAPDH*, glyceraldehyde 3-phosphate dehydrogenase; mRNA, messenger RNA; PCR, polymerase chain reaction; *Stat3*, signal transducer and activator of transcription 3.

In this study, real-time PCR was used to evaluate the differential expression of *Stat3*, *Bcl-xL*, and *Bax* in different groups. Following normalizing against the house-keeping gene, relative expression of *Stat3*, *Bcl-xL*, and *Bax* was 0.5067±0.045, 0.5933±0.0472, and 1.3933±0.1509 in the gene therapy combined with heating therapy group, respectively. In contrast, it was only 0.9467±0.035, 0.9417±0.0305, and 0.94±0.07 in the gene transfection-alone group, and only 0.7333±0.0568, 0.7367±0.0378, and 1.2167±0.1117 in the thermotherapy-alone group. mRNA expression of *Stat3* and *Bcl-xL* was downregulated, while that of *Bax* was upregulated in the combination therapy group and the thermotherapy-alone group, compared to the blank control group ($P<0.01$) (Figure 10). But, the relative expression of *Stat3, Bcl-xL*, and *Bax* in the gene transfection-alone group did not show significant changes compared to the blank control group ($P>0.05$) (Figure 10).

Furthermore, Western blot analysis also manifested that the protein levels of *p-Stat3* and *Bcl-xL* were downregulated, while the level of *Bax* was upregulated in the recombinant therapy group, compared to the other three groups ($P<0.01$) (Figure 11A and B). Meanwhile, we examined whether these therapy methods could alter the balance between proapoptotic Bax and antiapoptotic Bcl-xL proteins at the mitochondrial membrane and which therapy methods caused the greatest impact. As shown in Figure 11B, compared with the control group, groups (c) and (d) all resulted in a decrease in Bcl-xL and an increase in Bax, with an increase in the Bax/Bcl-xL ratio. However, the gene therapy combined with hyperthermia group had the greatest impact, inducing an increase in the Bax/Bcl-xL ratio to 2.716. This indicates that the combined therapy exhibited a rapid response to induce apoptosis of tumor cells.

Therefore, we proposed that the effects of this combination therapy on liver cancer in nude mice might occur through guanosine triphosphate c oxygen (ganciclovir triphosphate [GCV-TP]) suppression of Stat3 activation, which in turn blocks the *Stat3* signal transduction pathway, leading to downregulation of *Bcl-xL* and upregulation of *Bax*, thus inhibiting tumor growth.

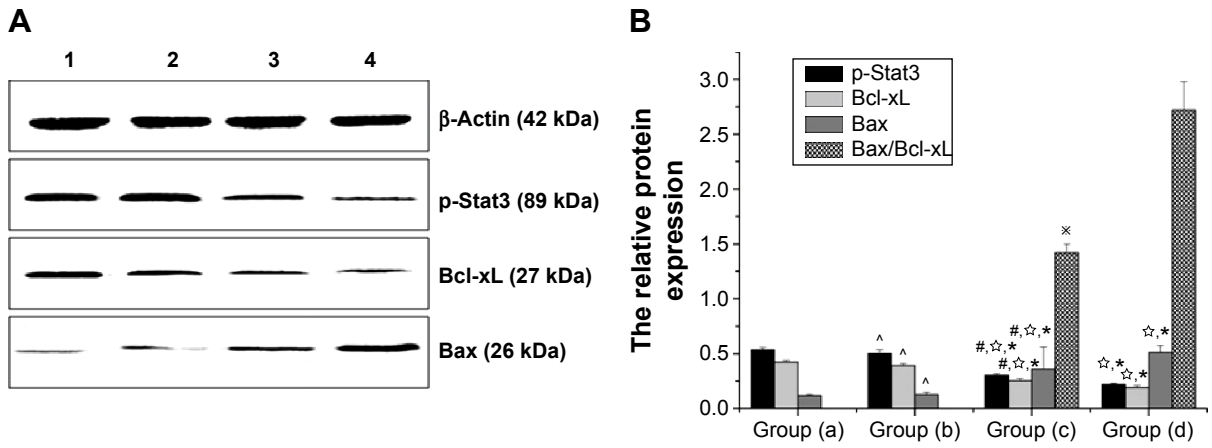

Figure 11 Western blot analyses of p-Stat3, Bcl-xL, and Bax protein expression. p-Stat3 =89 kDa; Bcl-xL =27 kDa; Bax =26 kDa; β-actin =42 kDa.

Notes: (**A**) Bax, pStat3, and Bcl-xL analysis by Western blot. Lane 1, blank control; lane 2, gene transfection-alone group; lane 3, the thermotherapy-alone group; lane 4, the combined therapy group. (**B**) Corresponding optical density ratio of p-Stat3/β-actin, Bcl-xL/β-actin, Bax/β-actin, and Bax/Bcl-xL. Data are reported as mean ± standard deviation (N=10). Group (a), blank control; group (b), gene transfection-alone group; group (c), the thermotherapy-alone group; group (d), the combined therapy group. *$P<0.05$, compared with blank control; ☆compared with gene transfection-alone group; #$P<0.05$, compared with the combined therapy group; ^$P>0.05$, compared with the blank control group; ※$P<0.05$, compared with the combined therapy group.

Abbreviations: Bax, bcl-2 associated X protein; Bcl-xL, B-cell lymphoma-extra large; Stat3, signal transducer and activator of transcription 3.

Conclusion

In this study, we explored a novel combination method of tumor therapy. We successfully transfected SMMC-7721 cells with pHsp 70-*HSV-TK*, resulting in sustained and stable transgenic expression. Furthermore, MZF-NPs were used as magnetic media for thermotherapy, and an Hsp 70 promoter was employed to strengthen the induction and modulation of *HSV-TK* gene expression by thermotherapy. Based on MFH, gene therapy and nanotechnology were combined organically. Both in vitro and in vivo experimental results indicated that that combined treatment provides a superior therapeutic effect compared with any of the therapies individually.

This novel combination of two therapeutic methods suggests the feasibility of this potential novel clinical approach to combination treatment of tumors; thus, further research is warranted.

Acknowledgments

This work was supported by the National Key Basic Research Program of China (973 Program) (2013 CB933904), the Natural Science Foundation of Jiangsu Province (BK2012335), and the National Natural Science Foundation of China (81271635, 81071881, and 81201131).

Disclosure

The authors report no conflicts of interest in this work.

References

1. Halim NSSA, Fakiruddin KS, Ali SA, et al. A comparative study of non-viral gene delivery techniques to human adipose-derived mesenchymal stem cell. *Int J Mol Sci*. 2014;15(9):15044–15060.
2. Carter JR, Keith JH, Fraser TS, et al. Effective suppression of dengue virus using a novel group-I intron that induces apoptotic cell death upon infection through conditional expression of the Bax C-terminal domain. *Virol J*. 2014;11(1):111.
3. Zhao W, Spatz S, Zhang Z, et al. Newcastle disease virus (NDV) recombinants expressing infectious laryngotracheitis virus (ILTV) glycoproteins gB and gD protect chickens against ILTV and NDV challenges. *J Virol*. 2014;88(15):8397–8406.
4. Leng Y, Wu C, Liu Z, et al. RNA-mediated gene silencing in the cereal fungal pathogen Cochliobolus sativus. *Mol Plant Pathol*. 2011;12(3):289–298.
5. Mehta V, Abi-Nader KN, Carr D, et al. Monitoring for potential adverse effects of prenatal gene therapy: use of large animal models with relevance to human application. *Methods Mol Biol*. 2012;291–328.
6. Ryffel B. Interleukin-12: role of interferon-γ in IL-12 adverse effects. *Clin Immunol Immunopathol*. 1997;83(1):18–20.
7. Sigel JE, Skacel M, Bergfeld WF, et al. The utility of cytokeratin 5/6 in the recognition of cutaneous spindle cell squamous cell carcinoma. *J Cutan Pathol*. 2001;28(10):520–524.
8. Manome Y, Kunieda T, Wen PY, et al. Transgene expression in malignant glioma using a replication-defective adenoviral vector containing the Egr-1 promoter: activation by ionizing radiation or uptake of radioactive iododeoxyuridine. *Hum Gene Ther*. 1998;9(10):1409–1417.
9. Hallahan DE, Mauceri HJ, Seung LP, et al. Spatial and temporal control of gene therapy using ionizing radiation. *Nat Med*. 1995;1(8):786–791.
10. Takahashi T, Namiki Y, Ohno T. Induction of the suicide HSV-TK gene by activation of the Egr-1 promoter with radioisotopes. *Hum Gene Ther*. 1997;8(7):827–833.
11. Walther W, Stein U, Schlag PM. Use of the human MDR1 promoter for heat-inducible expression of therapeutic genes. *Int J Cancer*. 2002;98(2):291–296.
12. Huang Q, Hu JK, Lohr F, et al. Heat-induced gene expression as a novel targeted cancer gene therapy strategy. *Cancer Res*. 2000;60(13):3435–3439.
13. Jordan A, Wust P, Scholz R, et al. Cellular uptake of magnetic fluid particles and their effects on human adenocarcinoma cells exposed to AC magnetic fields in vitro. *Int J Hyperthermia*. 1996;12(6):705–722.
14. Ren Y, Zhang H, Chen B, et al. Multifunctional magnetic Fe_3O_4 nanoparticles combined with chemotherapy and hyperthermia to overcome multidrug resistance. *Int J Nanomedicine*. 2011;7:2261–2269.
15. Huang HS, Hainfeld JF. Intravenous magnetic nanoparticle cancer hyperthermia. *Int J Nanomedicine*. 2013;8:2521–2532.
16. Liu L, Liu X, Xu Q, et al. Self-assembled nanoparticles based on the c (RGDfk) peptide for the delivery of siRNA targeting the VEGFR2 gene for tumor therapy. *Int J Nanomedicine*. 2014;9:3509–3526.
17. Santos J, Sousa F, Queiroz J, et al. Rhodamine based plasmid DNA nanoparticles for mitochondrial gene therapy. *Colloids Surf B Biointerfaces*. 2014;121:129–140.
18. Fargnoli AS, Mu A, Katz MG, et al. Anti-inflammatory loaded poly-lactic glycolic acid nanoparticle formulations to enhance myocardial gene transfer: an in-vitro assessment of a drug/gene combination therapeutic approach for direct injection. *J Transl Med*. 2014;12(1):171.
19. Tang Q, Zhang D, Gu N, et al. Synthesis and in vitro study of PEI-coated Mn-Zn ferrite-A novel gene vector. *J Fun Mater*. 2007;38(8):1268.
20. Tang Q, Zhang D, Cong X, et al. Using thermal energy produced by irradiation of Mn–Zn ferrite magnetic nanoparticles (MZF-NPs) for heat-inducible gene expression. *Biomaterials*. 2008;29(17):2673–2679.
21. Kuznetsov AA, Leontiev VG, Brukvin VA, et al. Local radiofrequency-induced hyperthermia using CuNi nanoparticles with therapeutically suitable Curie temperature. *J Magn Magnetic Mater*. 2007;311(1):197–203.
22. Arshak KI, Ajina A, Egan D. Development of screen-printed polymer thick film planner transformer using Mn–Zn ferrite as core material. *Microelectron J*. 2001;32(2):113–116.
23. Ito A, Shinkai M, Honda H, et al. Heat-inducible TNF-alpha gene therapy combined with hyperthermia using magnetic nanoparticles as a novel tumor-targeted therapy. *Cancer Gene Ther*. 2001;8(9):649–654.
24. Yuan CY, Tang QS, Zhang DS. Biocompatibility of $Mn_{0.4}Zn_{0.6}Fe_2O_4$ magnetic nanoparticles and their thermotherapy on VX2-carcinoma-induced liver tumors. *J Nanosci Nanotechnol*. 2015;15(1):74–84.
25. Huth S, Lausier J, Gersting SW, et al. Insights into the mechanism of magnetofection using PEI-based magnetofectins for gene transfer. *J Gene Med*. 2004;6(8):923–936.
26. Higashi K, Hazama S, Araki A, et al. A novel cancer vaccine strategy with combined IL-18 and HSV-TK gene therapy driven by the hTERT promoter in a murine colorectal cancer model. *Int J Oncol*. 2014;45(4):1412–1420.
27. Shao D, Li J, Xiao X, et al. Real-time visualizing and tracing of HSV-TK/GCV suicide gene therapy by near-infrared fluorescent quantum dots. *ACS Appl Mater Interfaces*. 2014;6(14):11082–11090.
28. Yin X, Yu B, Tang Z, et al. Bifidobacterium infantis-mediated HSV-TK/GCV suicide gene therapy induces both extrinsic and intrinsic apoptosis in a rat model of bladder cancer. *Cancer Gene Ther*. 2013;20(2):77–81.
29. National Institutes of Health. *Guide for the Care and Use of Laboratory Animals*. NIH Publication No 86-23, Revised 1996. Washington, DC: US Government Printing Office; 1996.
30. Litvak KJ, Schmittgen TD. Analysis of relative gene expression data using real-time quantitative PCR and the 2 (-Delta Delta C (T)) method. *Methods*. 2001;25(4):402–408.

31. Wallner KE, Li GC. Effect of drug exposure duration and sequencing on hyperthermic potentiation of mitomycin-C and cisplatin. *Cancer Res*. 1987;47(2):493–495.
32. Masunaga SI, Nishimura Y, Hiraoka M, et al. Efficacy of mild temperature hyperthermia in combined treatments for cancer therapy. *Thermal Med*. 2007;23(3):103–112.
33. Oei AL, Vriend LEM, Crezee J, et al. Effects of hyperthermia on DNA repair pathways: one treatment to inhibit them all. *Radiat Oncol*. 2015; 10(1):165.
34. Luo H, Xu M, Zhu X, et al. Lung cancer cellular apoptosis induced by recombinant human endostatin gold nanoshell-mediated near-infrared thermal therapy. *Int J Clin Exp Med*. 2015;8(6):8758–8766.
35. Saedi TA, Gharfourian S, Jafarlou M, et al. Berberis vulgaris fruit crude extract as a novel anti-leukaemic agent. *J Biol Regul Homeost Agents*. 2015;29(2):395–399.
36. Wani KD, Kadu BS, Mansara P, et al. Synthesis, characterization and in vitro study of biocompatible Cinnamaldehyde functionalized magnetite nanoparticles (CPGF NPs) for hyperthermia and drug delivery applications in breast cancer. *PLoS One*. 2014;9(9):e107315.
37. Dvorak HF. Vascular permeability factor/vascular endothelial growth factor: a critical cytokine in tumor angiogenesis and a potential target for diagnosis and therapy. *J Clin Oncol*. 2002;20(21):4368–4380.
38. Bromberg JF, Wrzeszczynska MH, Devgan G, et al. Stat3 as an oncogene. *Cell*. 1999;98(3):295–303.
39. Netchiporouk E, Litvinov IV, Moreau L, et al. Deregulation in STAT signaling is important for cutaneous T-cell lymphoma (CTCL) pathogenesis and cancer progression. *Cell Cycle*. 2014;13(21):3331–3335.
40. Yco LP, Mocz G, Opoku-Ansah J, et al. Withaferin A inhibits STAT3 and induces tumor cell death in neuroblastoma and multiple myeloma. *Biochem Insights*. 2014;7:1–13.
41. Lin WL, Lai DY, Lee YJ, et al. Antitumor progression potential of morusin suppressing STAT3 and NFκB in human hepatoma SK-Hep1 cells. *Toxicol Lett*. 2015;232(2):490–498.